Evolution of the Spin Hall Effect in Pt Nanowires: Size and Temperature Effects

Laurent Vila,[1] Takashi Kimura,[1,2] and YoshiChika Otani[1,2,*]

[1]*Institute for Solid State Physics, University of Tokyo, Kashiwanoha, Kashiwa, Chiba 277-8581, Japan*
[2]*Frontier Research System, RIKEN, Wako, Saitama 351-0198, Japan*

(Received 28 August 2007; published 29 November 2007)

We have studied the evolution of the spin Hall effect (SHE) in the regime where the material size responsible for the spin accumulation is either smaller or larger than the spin diffusion length. Lateral spin valve structures with Pt insertions were successfully used to measure the spin absorption efficiency as well as the spin accumulation in Pt induced through the spin Hall effect. Under a constant applied current the results show a decrease of the spin accumulation signal is more pronounced as the Pt thickness exceeds the spin diffusion length. This implies that the spin accumulation originates from bulk scattering inside the Pt wire and the spin diffusion length limits the SHE. We have also analyzed the temperature variation of the spin Hall conductivity to identify the dominant scattering mechanism.

DOI: 10.1103/PhysRevLett.99.226604 PACS numbers: 72.25.Ba, 72.25.Mk, 75.70.Cn, 75.75.+a

Recently a long-standing prediction of the spin Hall effect (SHE) [1–3] has been verified by means of both optical [4–7] and magnetotransport [8–10] measurements. The SHE originates from the spin-orbit coupling, which relates the spin of an electron to its momentum, producing a spin current in the direction transverse to the flow of electrons and a spin accumulation at lateral sample boundaries. This is the direct SHE (DSHE) where unpolarized charge currents are converted into pure spin currents with zero net charge flow. There is also the inverse effect called inverse SHE (ISHE) where pure spin currents can be converted into charge currents by the spin-orbit interaction. The SHE is therefore regarded as a new tool for generating and detecting spin currents, crucial issues for future *spintronics*, that in principle does not require ferromagnetic elements and/or external magnetic field.

The SHE induced spin accumulation in semiconductors (SCs) have drawn much attention because of its compatibility with conventional complementary metal-oxide-semiconductor device technology. However, up to now SCs have exhibited very small SHE and no electrical detection has been reported yet. On the contrary Pt metal has been successfully used to detect the SHE even at room temperature, exhibiting the largest spin Hall conductivity reported so far [9]. The possible origins of the SHE can be classified in two categories, intrinsic and extrinsic, depending on the dominant influence of either band structure or impurities [11]. The SHE is also expected to be strongly geometry dependent. In metals like Pt, the SHE may be mainly attributable to extrinsic mechanisms such as the side jump and the skew scattering, which are responsible for the anomalous Hall effect in ferromagnets. The different sign of the side jump or the skew scattering angle for the two spin channels results in the transverse spin current and spin accumulation at lateral boundaries. One should also remark here that recent theoretical analysis based on the first-principles band calculation strongly suggests that the origin of the large SHE in Pt is of intrinsic nature [12]. Thus it is important to perform systematical experiments in order to better understand the origin of the SHE.

The first electrical detection scheme, originally proposed by Takahashi and Maekawa [13], was successfully applied for aluminum by Valenzuela *et al.* [8]. But this method is not suitable for the material with a nanometer scale spin diffusion length l_{sf} due to strong spin-orbit interaction. Therefore in a previous study [9] we have demonstrated a new device design where the Cu wire transfers accumulated spins at the interface between ferromagnetic detector (or injector) and Pt with negligible relaxation for both DSHE and ISHE measurements. In the previous study, we assumed that the induced spin current at the Cu/Pt interface was completely absorbed by the Pt wire because of its small spin resistance. However, the absorption efficiency of the spin current may depend on the device geometry and the temperature. Therefore, we further modified the previous design to a lateral spin valve (LSV) structure with a Pt insertion, which enables us to determine explicitly the magnitude of the absorbed spin current. Thereby the spin Hall conductivity for the Pt wire can be well evaluated.

Our device is based on the LSV geometry [14–16] where a Pt wire is inserted, which can be either a spin current source for DSHE or a spin current absorber for ISHE experiments. The devices are prepared by means of conventional e-beam lithography, electron gun evaporation (base pressure $\sim 10^{-8}$ Torr) and a lift-off process. The scanning electron image of a typical device is shown in Fig. 1(a). A Pt wire 100 nm wide (w_{Pt}) with a thickness t_{Pt} varied from 5 to 20 nm is in ohmic contact with a Cu wire running between two Permalloy (Py) wires 100 nm in width and 30 nm in thickness. The dimensions of the Cu wire are 160 nm in width and 100 nm in thickness. Prior to Cu evaporation a careful Ar ion beam etching is carried out for cleaning the surface to obtain highly transparent Ohmic contacts [16]. The measurements are carried out by using ac lock-in amplifier and a He flow cryostat. The magnetic

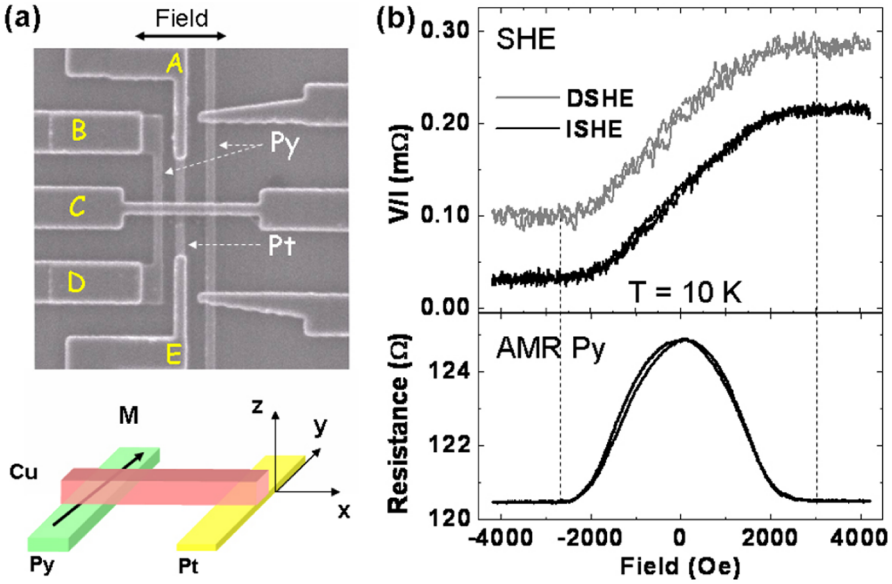

FIG. 1 (color online). (a) SEM image of the typical device for SHE measurements and an illustration of the device. (b) Direct and Inverse SHE (DSHE and ISHE) recorded at $T = 10$ K using a device with $t_{\mathrm{Pt}} = 20$ nm, altogether with the AMR from the Py wire measured on the same condition. DSHE measurement corresponds to V_{BC}/I_{AE}, and ISHE to V_{EA}/I_{BC}; with V the voltage, I the applied current; A, B, C and E are the contact leads as denoted in the SEM image.

fields between -4 kOe and $+4$ kOe are applied in the plane of the substrate.

The charge to spin conversion induced by SHE obeys a relation given by the vector product, $\boldsymbol{J}_s \propto \boldsymbol{S} \times \boldsymbol{J}_c$ with $\boldsymbol{J}_{s(c)}$ the spin (charge) current density and $\boldsymbol{S}$ the spin orientation. Similarly the spin to charge conversion obeys the reciprocal relation, $\boldsymbol{J}_c \propto \boldsymbol{S} \times \boldsymbol{J}_s$. In the case of DSHE, the spins aligned along the x axis of the unpolarized charge current in the Pt wire are therefore accumulated in the vicinity of the top or bottom surface according to the spin orientation. The accumulated spins are transferred through the Cu wire to the Py spin detector in Fig. 1(a). The magnitude of the spin accumulation is measured as the spin signal $R_S = V_{BC}/I$, where V_{BC} is the voltage between the contact leads B and C and I ($= 80$ μA) is the current flowing in the Pt wire through contact leads A and E. When the magnetic field is applied along the x axis, the spin signal R_S exhibits a linear increase and gets saturated above the saturation field, reflecting a hard axis magnetization process of Py wire. This magnetization process is separately confirmed by the anisotropic magnetoresistance measurement as in the bottom of Fig. 1(b). The overall change ΔR_S in the spin signal is about 0.18 mΩ.

In the case of the ISHE curve in Fig. 1(b), the spin current is injected by flowing a current of 240 μA between B and C. The voltage is induced between E and A as a result of the spin to charge conversion since the spin current is preferentially absorbed in the Pt wire along the z axis. From the field variation, the overall change in charge accumulation signal ΔR_{SHE} is also determined to be 0.18 mΩ which is equal to ΔR_S in the DSHE, indicating the reciprocity of the behavior. The angular variation of the spin and charge accumulation signals measured with rotating the applied field direction assure the relation among the vectors $\boldsymbol{J}_s$, $\boldsymbol{J}_c$, and $\boldsymbol{S}$.

The efficiency of the spin absorption is studied by nonlocal spin valve (NLSV) measurements detailed in [16]. For this measurement the magnetic field is applied along the Py wires. For all devices the center to center distance d between the Py wires is fixed to 800 nm. The inset in Fig. 2 compares the NLSV signals measured at 5 K for the devices with and without a Pt insertion between the two Py electrodes. The NLSV signal for $I \sim 240$ μA clearly decreases once the Pt is inserted, indicating the spin current absorption into the Pt wire, in good agreement with previous experiments [16]. For all the devices the NLSV signal is almost a factor of 5 decreased by the Pt insertion from 5 K to room temperature (RT). We now define the ratio η, which is the ratio of the spin signal with and without a Pt insertion, $\Delta R_{\mathrm{SV}}^{\mathrm{with}}$ and $\Delta R_{\mathrm{SV}}^{\mathrm{ref}}$, respectively. By solving the one dimensional spin diffusion model with transparent interfaces, η can be calculated as

$$\eta \equiv \frac{\Delta R_{\mathrm{SV}}^{\mathrm{with}}}{\Delta R_{\mathrm{SV}}^{\mathrm{ref}}} \approx \frac{\frac{R_{\mathrm{Pt}}}{R_{\mathrm{Cu}}} \sinh(d/l_{\mathrm{sf}}^{\mathrm{Cu}})}{\cosh(d/l_{\mathrm{sf}}^{\mathrm{Cu}}) + \frac{R_{\mathrm{Pt}}}{R_{\mathrm{Cu}}} \sinh(d/l_{\mathrm{sf}}^{\mathrm{Cu}}) - 1}. \quad (1)$$

Here, R_{Pt} and R_{Cu} are the spin resistances for the Pt and Cu wires, respectively. $l_{\mathrm{sf}}^{\mathrm{Cu}}$ is the spin diffusion length for the Cu wire.

Interesting is that the ratio η varies from 0.35 at 5 K to 0.2 at RT irrespective of the Pt thickness. This implies that the spin absorption into the Pt wire takes place only at the

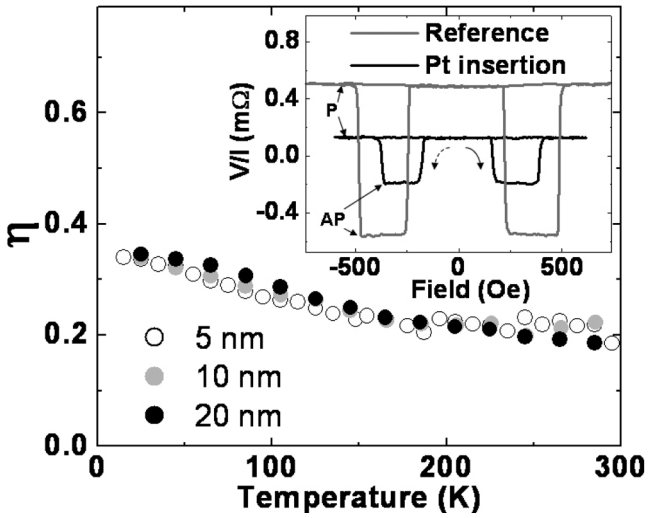

FIG. 2. Temperature evolution of the spin absorption for Pt wires with $t_{Pt} = 5$, 10 and 20 nm and $w_{Pt} = 100$ nm. The inset shows nonlocal spin valve signals measured at 5 K for LSVs with and without Pt insertion ($t_{Pt} = 5$ nm) clearly indicating parallel (P) and antiparallel (AP) states.

top interface between Pt and Cu wires. The reason for this may be due to the anisotropic Ar milling process which left side surfaces of the Pt insertion uncleaned. The η deduced from the experimental results yields the spin resistance of the Pt wire as 0.22 Ω both at RT and 5 K. Since the spin resistance R_{Pt} of the Pt wire is given by $2l_{sf}^{Pt}/(\sigma_{Pt}S)$, where σ_{Pt} and S are the conductivity for the Pt and the effective cross section for the spin current in the Pt wire, l_{sf}^{Pt} can be estimated as 14 nm at 5 K and 10 nm at RT, in good agreement with the value of 14 ± 6 nm at 4 K reported by Kurt *et al.* [17].

Figures 3(a)–3(c) represent the field dependences of the ISHE with different Pt thicknesses of 5, 10 and 20 nm measured at RT. Here, the distance d is 350 ± 20 nm. We

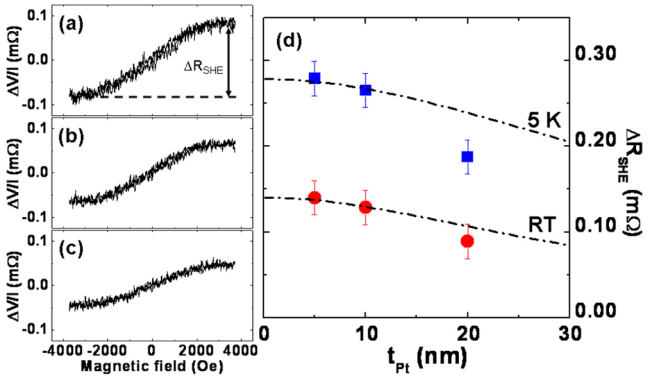

FIG. 3 (color online). Inverse spin Hall effect measured at RT for (a) $t_{Pt} = 5$ nm, (b) 10 nm and (c) 20 nm. The distance d is of the order of 350 nm. (d) ΔR_{SHE} as a function of t_{Pt} at 5 K and RT for $d = 350$ nm. The dashed lines are the calculated evolution of ΔR_{SHE} using Eq. (2).

have studied about 20 devices of $t_{Pt} = 5$, 10, and 20 nm, with different values of d varied from 250 to 500 nm to evaluate the thickness dependence of the SH signal. All the devices exhibit a gradual decrease of DSHE and ISHE with d proportional to $\sinh^{-1}(d/l_{sf}^{Cu})$ due to the spin relaxation in the Cu wire. Interestingly, a clear systematic decrease in ΔR_{SHE} with t_{Pt} has been observed in the temperature range from 5 K to RT. Figure 3(d) summarizes the ΔR_{SHE} values at RT and 5 K obtained for the distance d of 350 nm. There is a very small decrease in ΔR_{SHE} when the thickness t_{Pt} is increased from 5 to 10 nm. Remarkable is that there is a more pronounced decrease when the thickness is further increased from 10 to 20 nm. This can be understood as follows. The spin accumulation at the top surface of the Pt due to the DSHE effectively takes place in the Pt while the thickness $t_{Pt} < l_{sf}^{Pt}$. Once t_{Pt} exceeds l_{sf}^{Pt}, the spin accumulation should not increase under the condition of the constant current. For the ISHE, the vertical penetration of the spin current from Cu into Pt is limited by l_{sf}^{Pt}, leading to the same ΔR_{SHE} as ΔR_S. For more quantitative analyses, we calculate the thickness dependence of the spin accumulation ΔV_S due to DSHE at the top surface of the Pt wire. Since the spin relaxation in the Cu wire does not depend on t_{Pt}, the thickness dependence of ΔR_S or ΔR_{SHE} is proportional to ΔV_S. Using the homogeneous spin Hall conductivity σ_{SHE} in the Pt wire with open circuit condition, ΔV_S can be calculated as

$$\Delta V_S = \frac{\sigma_{SHE} I_C}{\sigma_{Pt}^2} \frac{l_{sf}^{Pt}}{w_{Pt} t_{Pt}} \frac{\exp(t_{Pt}/l_{sf}^{Pt}) - 1}{\exp(t_{Pt}/l_{sf}^{Pt}) + 1}, \quad (2)$$

where I_C is the excitation current flowing in the Pt wire. As shown in Fig. 3(d), Eq. (2) with $l_{sf}^{Pt} = 10$ nm at RT and 14 nm at 5 K, which are deduced from the absorption experiment mentioned previously, fairly well reproduce the thickness evolution of ΔR_{SHE}. The data can be well reproduced when slightly reducing l_{sf}^{Pt} to 7 nm and 8 nm for RT and 5 K, respectively. These features strongly support the bulk origin of the DSHE and ISHE.

Finally, we discuss the temperature dependence of the spin Hall conductivity. The spin Hall conductivity σ_{SHE} can be calculated as ([3,8,9])

$$\sigma_{SHE} = w_{Pt} \sigma_{Pt}^2 \frac{I_c \Delta R_{SHE}}{I_s}, \quad (3)$$

with the parameters in [18] to estimate the ratio I_c/I_s of charge to spin currents. The obtained value of σ_{SHE} is 330 S/cm at RT (unit equivalent to $\Omega^{-1}\,\mathrm{cm}^{-1}$), which is larger than that in the previous experiment. This is because the assumption of the complete spin current absorption into the Pt wire in the previous analysis led to underestimate the spin Hall conductivity.

Using Eq. (3) with the temperature dependences of ΔR_{SHE} and the spin resistances for Pt, Cu and Py, we can compute σ_{SHE}. As shown in the inset of Fig. 4, the temperature dependence exhibits a very small variation of

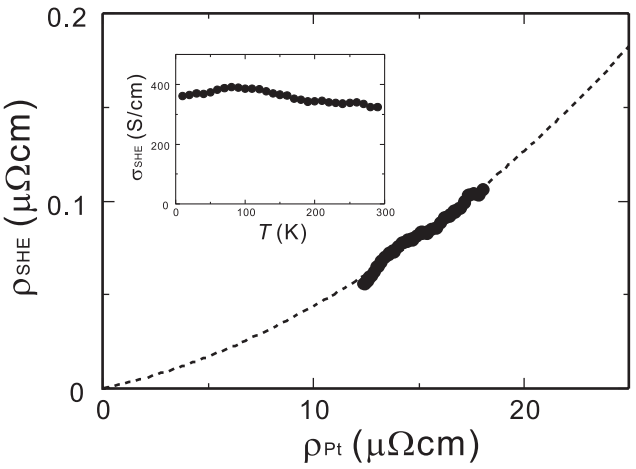

FIG. 4. Evaluated ρ_{SHE} as a function of the longitudinal resistivity ρ_{Pt} for the device in Fig. 3(a) with $t_{Pt} = 5$ nm and $d = 325$ nm. Fitting to the polynomial yields $\rho_{SHE} = 2.5 \times 10^{-3}\rho_{Pt}(\mu\Omega\,\mathrm{cm}) + 1.9 \times 10^{-4}[\rho_{Pt}(\mu\Omega\,\mathrm{cm})]^2$. The inset represents the calculated σ_{SHE} as a function of temperature using Eq. (3).

σ_{SHE} around 350 S/cm. It should be noted that the change in σ_{SHE} is much smaller than that in [12] obtained from band structure calculation. Our values of σ_{SHE} are smaller at low temperatures but larger at RT (2000 S/cm and 240 S/cm in [12] for low temperature and RT, respectively). This difference could be due to the dominant contribution of impurities compared to the band structure considerations in the Pt wires. In Fig. 4 the SH resistivity ($\rho_{SHE} \approx \frac{\sigma_{SHE}}{\sigma_{Pt}^2}$) is likely to evolve in a quadratic form with the Pt resistivity ρ_{Pt} with ρ_{Pt} in this temperature range. This is expected evolution for side jump origin of the SHE.

In conclusion we have studied the evolution of the spin Hall effect in Pt wires in the regime where the size responsible for the spin accumulation is either smaller or larger than the spin diffusion length. Under the constant current the pronounced decrease in the SHE for $t_{Pt} > l_{sf}^{Pt}$ demonstrates that the SHE is induced by bulk scattering inside the Pt wire. The analyses on the spin Hall conductivity of the Pt wires suggest a side jump origin of the SHE. These results will provide important information in determining the optimum geometry for the SHE.

We thank Professors Y. Iye and S. Katsumoto of ISSP, Univ. of Tokyo for the use of the lithography facilities.

*yotani@issp.u-tokyo.ac.jp

[1] M. I. Dyakonov and V. I. Perel, Phys. Lett. **35**, 459 (1971).
[2] J. E. Hirsch, Phys. Rev. Lett. **83**, 1834 (1999).
[3] S. Zhang, Phys. Rev. Lett. **85**, 393 (2000).
[4] Y. K. Kato, R. S. Myers, A. C. Gossard, and D. D. Awschalom, Science **306**, 1910 (2004).
[5] N. P. Stern, S. Ghosh, G. Xiang, M. Zhu, N. Samarth, and D. D. Awschalom, Phys. Rev. Lett. **97**, 126603 (2006).
[6] J. Wunderlich, B. Kaestner, J. Sinova, and T. Jungwirth, Phys. Rev. Lett. **94**, 047204 (2005).
[7] V. Sih, R. C. Myers, Y. K. Kato, W. H. Lau, A. C. Gossard, and D. D. Awschalom, Nature Phys. **1**, 31 (2005).
[8] S. O. Valenzuela and M. Tinkham, Nature (London) **442**, 176 (2006).
[9] T. Kimura, Y. Otani, T. Sato, S. Takahashi, and S. Maekawa, Phys. Rev. Lett. **98**, 156601 (2007).
[10] E. Saitoh, M. Ueda, H. Miyajima, and G. Tatara, Appl. Phys. Lett. **88**, 182509 (2006).
[11] For recent theoretical reviews on the SHE in SCs see J. Schliemann, Int. J. Mod. Phys. B **20**, 1015 (2006); H. A. Engel, E. I. Rashba, and B. I. Halperin, arXiv:cond-matt/0603306.
[12] G. Y. Guo, S. Murakami, T.-W. Chen, and N. Nagaosa, arXiv:cond-mat/07050409.
[13] S. Takahashi and S. Maekawa, Physica (Amsterdam) **437C**, 309 (2006).
[14] F. J. Jedema, A. T. Filip, and B. J. van Wees, Nature (London) **410**, 345 (2001).
[15] F. J. Jedema, M. S. Nijboer, A. T. Filip, and B. J. van Wees, Phys. Rev. B **67**, 085319 (2003).
[16] T. Kimura, J. Hamrle, and Y. Otani, Phys. Rev. B **72**, 014461 (2005).
[17] H. Kurt, R. Loloee, K. Eid, W. P. Pratt, Jr., and J. Bass, Appl. Phys. Lett. **81**, 4787 (2002).
[18] From independant measurements l_{sf}^{Cu}, R_{Cu}, R_{Py} and p were estimated to be, respectively, 500 nm, 1.3 Ω, 0.09 Ω, 0.2 at RT and 1500 nm, 1.7 Ω, 0.13 Ω, 0.35 at 5 K.